JTTEE5 17:228–233
DOI: 10.1007/s11666-008-9168-2
1059-9630/$19.00 © ASM International

Tensile Test Specimens with a Circumferential Precrack for Evaluation of Interfacial Toughness of Thermal-Sprayed Coatings

Akio Kishi, Seiji Kuroda, Tadanobu Inoue, Takeshi Fukushima, and Hisami Yumoto

(Submitted August 10, 2007; in revised form January 8, 2008)

A new testing procedure to evaluate the interfacial toughness of thermal-sprayed coatings has been developed. The newly designed test specimen is a modification of the pin test with an artificially introduced weak interface, which is expected to open up easily under tensile loading and act as a circumferential precrack along the interface between a coating and the substrate. This configuration makes it possible to calculate the stress intensity factor K_{Int} at the tip of the precrack, which can be expressed as $K_{Int} = \sigma_0\sqrt{\pi a}F_I(a/R)$, where σ_0 is the apparent average stress, a the crack length, R the specimen radius, and F_I the geometrical correction function. Finite-element analysis was carried out to calculate the correction function F_I for various values of a/R. In the experiments, the flat surface of a pin was grit-blasted and a ring-shaped area from the periphery was covered with carbon using a pencil and set into a mating dice. SUS316L stainless steel was plasma-sprayed onto the flat surface of the pin and the dice. Then, tensile load was applied to the pin to break the weak interface containing the carbon and finally the unmodified coating-substrate interface. The load required to pull out the pin was measured for various specimen parameters such as a and R. The results indicate that the adhesion of the tested coatings can be represented by interface toughness of 1.9 ± 0.1 MPa $m^{1/2}$. As a consequence, this testing procedure can be considered as a viable method to evaluate adhesion of a thermal-sprayed coating on a substrate.

Keywords adhesion of TS coatings, APS coatings, coating-substrate interaction

1. Introduction

Adhesion strength of thermal-sprayed coatings is of crucial importance in many industrial applications, as it influences the performance of produced coatings such as impact resistance, fatigue life, and even corrosion resistance (Ref 1, 2). Various processing parameters are known to affect adhesion of sprayed coatings such as surface preparation of substrate, temperature of substrate during spraying, and residual stresses (Ref 3-6). There are a number of testing methods to evaluate adhesion strength or interfacial fracture toughness of coatings such as pin test, shear adhesion test, bending test, peeling test and double cantilever beam (DCB) test, interfacial indentation test, and so on (Ref 7-15). Among them, tensile adhesion test is most commonly used because the specimen preparation and the experimental procedure are relatively easier than the other methods. In the conventional tensile adhesion testing methods such as those standardized in ISO 14916:1999, ASTM C633-79, and JIS H 8402:2004, some adhesive resin is used to bond a dolly to apply a load to the coating (Ref 16-18). Even though this type of testing has been most widely used due to the relatively simple configuration and procedure, there are cases in which measurement of adhesive strength of the sprayed coating is difficult. A typical example is HVOF-sprayed cermet coatings, whose adhesion strength often exceeds the strength of normally available adhesives (Ref 19). Pin-test specimen is attractive since the maximum measurable strength is not limited by the adhesive used.

Inoue et al. studied a pin-test specimen from the viewpoint of stress singularity that appears at the edge of the pin (Ref 20). Powders of 80Ni-20Cr, CoNiCrAlY, and ZrO_2-$8Y_2O_3$ were sprayed onto the pin specimens of cast iron (FCD45) and SUS304 stainless steel with various diameters and coating thicknesses. Then, the stress intensity factor at the edge of a pin was calculated by finite-element method and used to analyze the experimental results. It was found that the stress intensity at the edge is a more consistent criterion for the tensile failure under the testing configuration. This technique was applied to HVOF metallic and cermet coatings in our laboratory. However, the edge of a pin was rounded during grit blasting and more severely during spraying due to the collision of high-velocity HVOF-sprayed particles. As a consequence, the calculated stress intensity factor

Akio Kishi and **Hisami Yumoto**, Tokyo University of Science, 2641, Yamasaki, Noda, Chiba 278-8510, Japan; **Akio Kishi**, Toyota Motor Corporation, Toyota-shi, Aichi Prefecture, Japan; and **Seiji Kuroda**, **Tadanobu Inoue**, and **Takeshi Fukushima,** National Institute for Material Science, 1-2-1, Sengen, Tsukuba, Ibaraki, 305-0047, Japan. Contact e-mail: KURODA.Seiji@nims.go.jp.

was not valid for tensile failure of the coating-substrate interface (Ref 21).

Another problem of the conventional tensile testing is that the failure stress tends to scatter significantly and a large number of testing methods are required to obtain statistically meaningful results. This is possibly because of the lack of control over the morphology of the substrate surface at the circumferential edge of a cylindrical specimen in the micrometer scale, where the stress concentration is expected to be the highest. Qian et al. proposed a tensile toughness test incorporating a crack embedded within the coatings, which was prepared by introducing a thin circular carbon layer during fabrication of thermal barrier coating (TBC) (Ref 22). They calculated the energy release rates as a function of the embedded-crack radius placed at different locations in TBC. It was demonstrated that when the crack was located within the ceramic topcoat, fracture occurred along the plane of the crack without kinking and the measured critical stress showed least scattering, giving a value of 1.0 J/m^2 as the critical strain energy release rate of the ceramic topcoat.

In view of these, therefore, a new type of pin-test specimen with an artificially introduced crack was designed in the present study for which the geometry of the critical part is not affected by grit blasting or coating formation. The test specimen incorporates an artificially introduced weak interface, which is expected to act as a circumferential precrack between a coating and the underlying substrate. Numerical analysis was carried out to characterize the stress field at the crack front, which is expected to control the initiation and subsequent tensile failure of the coating upon loading. Several test specimens with different crack lengths and pin diameters were prepared with 316L stainless steel coating applied by atmospheric plasma spraying (APS). Results of the tensile test were analyzed in terms of two stress criteria as well as the calculated stress intensity factor at the crack front.

2. Experimental Procedure

2.1 Modified Tensile Adhesion Test

A schematic of the new tensile test is shown in Fig. 1. A tapered pin-test specimen is designed in such a way that when it is set into the mating dice, the flat surface of the pin and that of the dice make a plane surface. First, the coupled pin and the dice are grit blasted with alumina and the pin is pulled out. Then, a carbon layer of width a from the periphery is placed onto the grit-blasted surface of a pin using a pencil and a lathe (Step 1), which will weaken the bonding of the coating to be sprayed onto the pin surface and is expected to behave as a precrack during the subsequent tensile test (Ref 22). The pin is then set back on to the dice and a coating is formed by spraying it onto the upper surface of the pin and the dice to the desired thickness (Step 2). After spraying, a backing plate is bonded to the coating surface (Step 3) and the pin is pulled out to measure the failure load (Step 4).

In the experiments, the pin radius R at the top was either 5 or 10 mm; the width a of the carbon layer was 1, 2, or 6 mm (6 mm was for the 10-mm pin only); the coating thickness was aimed at 400 μm; and the clearance Δr between the pin and the surrounding dice was 100 μm. The material for the pin and the dice was a low-carbon steel with a tensile strength of 400 MPa (JIS SS400). A thermosetting adhesive (CIBA-GEIGY: AV118) was used to bond the backing plate; the specimens were heated

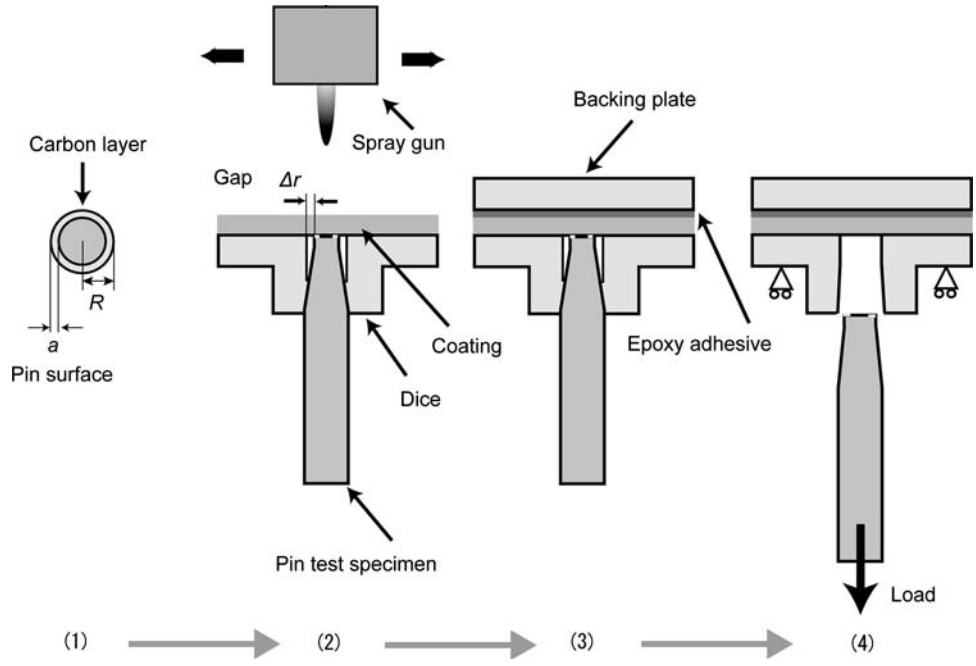

Fig. 1 Procedure and configuration of the pin test

at 423 K for 2 h to harden the adhesive and then cooled down to room temperature. A tensile-test machine (Shimadzu: AUTOGRAPH AG-100 kND) was used for applying tensile load to pull out the pin and the rate of displacement was 0.5 mm/min and the displacement-load curve and the maximum load at failure were recorded automatically in a PC.

2.2 Spraying Condition and Coating Material

Plasma-spraying equipment (Praxair: SG-100) was used to spray coatings. Gas-atomized spherical stainless steel SUS316L powder (Fe balance, Cr: 16.8%, Ni: 10.8%, Mo: 2.05%, N: 0.131%, O: 0.026%, particle size: 20-53 μm) was sprayed under the conditions listed in Table 1.

3. Analysis of the Problem: Numerical Procedure and Its Results

3.1 Theoretical Analysis

In the subsequent analysis, it is assumed that (1) in the tensile test, the region with the carbon layer at the coating-substrate interface debonds first at a relatively low load, (2) debonding does not continue to proceed into the region without carbon and hence the debonded region acts as a ring-shaped precrack, and (3) failure of the unmodified coating-substrate interface occurs when the stress intensity factor K_{Int} at the crack tip reaches a critical value K_C, which should be an intrinsic property of the coating-substrate interface prepared under a set of processing conditions, but should not depend on the geometry of the test specimens such as the pin radius, coating thickness, and the length of the precrack. Equation (1) shows the relationship of K_{Int} with the far-field average stress σ_0 and the size a of the precrack based on fracture mechanics. The correction function F_I is expected to be a function of a/R but needs to be calculated analytically or numerically.

$$K_{Int} = \sigma_0 \sqrt{\pi a} F_I(a/R) \quad \text{(Eq 1)}$$

where F_I is correction function; R is specimen radius; and a is crack length.

On the other hand, K_{Int} at the crack front can be calculated by Eq 2 as proposed by Yuuki (Ref 23).

$$K_{Int} = \lim_{r \to 0} \sqrt{2\pi r(\sigma_{zz}^2 + \tau_{rz}^2)} \quad \text{(Eq 2)}$$

where r is distance from the crack tip; σ_{zz} is normal stress in the vicinity of the crack tip; and τ_{rz} is shear stress in the vicinity of the crack tip.

Table 1 List of spraying conditions

Spray parameter	Value
Plasma gas flow, L/min	Ar, 45
Spraying distance, mm	100
Arc current, A	700
Arc voltage, V	30
Traverse speed of gun, mm/s	300

Therefore, if we characterize the stress field in the vicinity of the crack tip introduced between a sprayed coating and the substrate in the test specimen for a unit stress σ_0, it is possible to obtain K_{Int} using the relationship shown by Eq 2, from which $F_I(a/R)$ can be obtained by doing analysis for various values of a and R. Numerical approach using finite-element analysis is carried out for this purpose.

3.2 Numerical Analysis

Parameters used in the FE analysis are shown in Table 2. Effects of changing the pin radius R and the crack length a are examined. Materials for the substrate/coating are SS400/SUS316L corresponding to the experiments. The elastic moduli (E_b, E_c) of the substrate and the coating used in the analysis are also shown. The elastic modulus for SUS316L is about 200 GPa, but it is set as 100 GPa in the analysis since it is known to become about one-third to a half for plasma-sprayed coatings of the corresponding bulk value due to the existence of porosity, oxide inclusion, etc. (Ref 24). Poisson's ratio for both the substrate and coating is assumed to be 0.3.

Figure 2 shows the mesh division of a pin-test specimen used in the FE analysis. The analysis code used is ABAQUS/Standard ver.5.8, and the elements used are the 8-node quadratic element in an axisymmetric model. The mesh in the vicinity of a crack tip is divided most finely because the stress field is expected to change most sharply

Table 2 Diameter of pin, crack length, and elastic modulus used in the FE analysis

Substrate/coating	Diameter of pin, mm	Crack length, mm	E_b, GPa	E_c, GPa
SS400/SUS316L	10	0.25, 0.5, 1, 2	200	100
	20	1, 2		

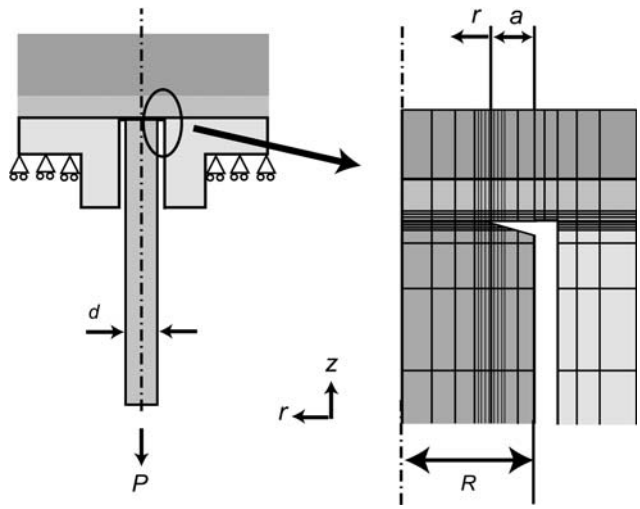

Fig. 2 FEM mesh division used to analyze the stress field near the crack tip of a pin-test specimen

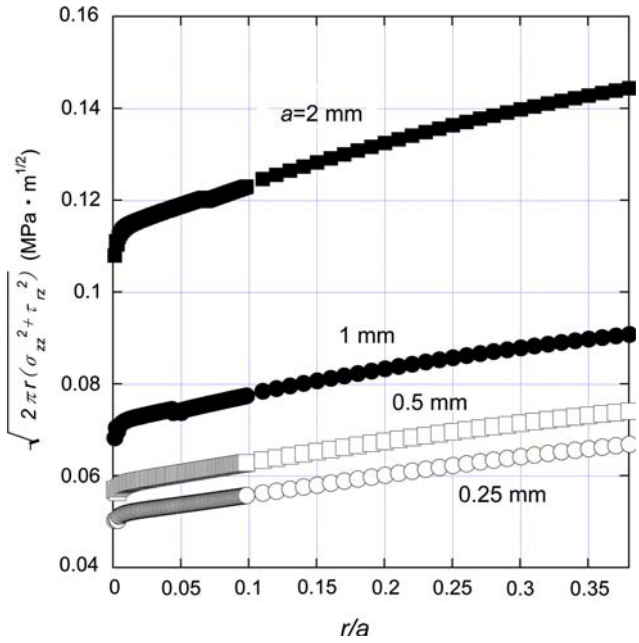

Fig. 3 Behavior of the function $\sqrt{2\pi r(\sigma_{zz}^2 + \tau_{rz}^2)}$ with respect to r/a for four different values of crack length a for $R = 5$ mm. This graph is used for the extrapolation method for obtaining the correction factor F_I that is required for calculating K_{Int}

in that region. The smallest mesh size is 1 μm and the numbers of elements and nodes are in the range between 62125 and 93200 and between 187796 and 281467, respectively.

Figure 3 shows the behavior of the function $\sqrt{2\pi r(\sigma_{zz}^2 + \tau_{rz}^2)}$ as a function of r/a for four different values of crack length a for $R = 5$ mm. The stress intensity K_{Int} was obtained from the y-intercepts of Fig. 3, and F_I, which was calculated by substituting K_{Int} into Eq 1, is shown in Fig. 4 for $R = 5$ mm as well as for $R = 10$ mm. The result shows that the correction function F_I can be evaluated in terms of a/R as expected.

4. Results

Figure 5 shows an example of the nominal stress vs. displacement curve in the tensile pin test. Once loading was done, the stress curve first increased almost linearly with displacement, then, it passed through a plateau at about 3 MPa. Then, the stress increased again almost linearly till failure occurred at stress σ_c. The value of 3 MPa in this graph roughly corresponds to the stress required to debond a pin whose surface was fully covered by a carbon layer before spraying. It is, therefore, reasonable to assume that the plateau in the figure represents the debonding process at the weakened coating-substrate interface made by the carbon layer.

Figure 6(a) and (b) shows the results of all the tests with the length a of a precrack at 1, 2, and 6 mm and the pin radius R of 5 and 10 mm. The fracture stress σ_c was obtained by dividing the applied load by the total pin

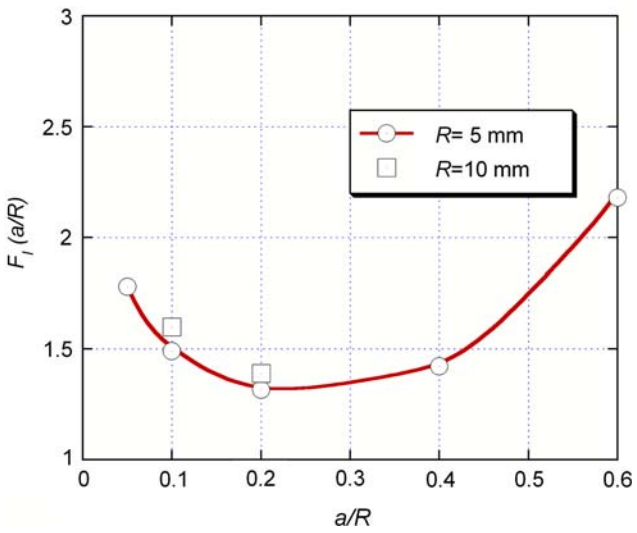

Fig. 4 Correction function F_I obtained by the extrapolation method as shown in Fig. 3

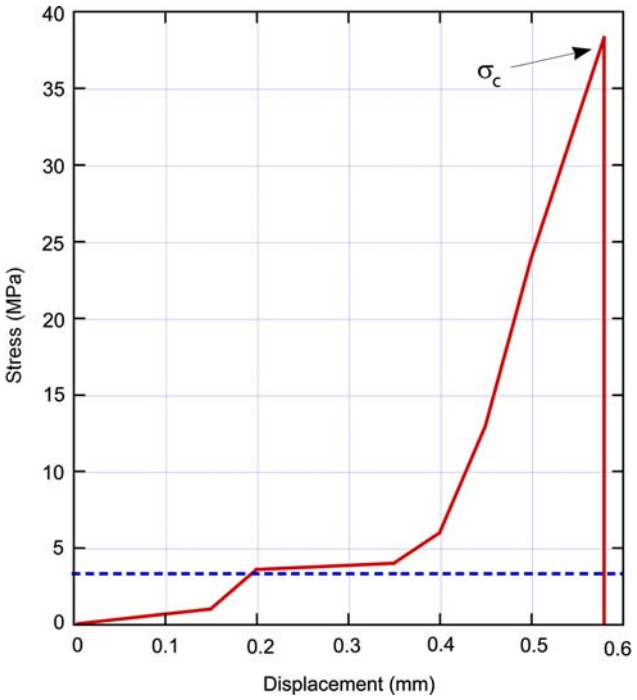

Fig. 5 Example of nominal stress vs. displacement curve obtained in the test

surface area, whereas the fracture net stress σ_n was obtained by dividing the failure load by the area of unmodified interface not covered by a carbon layer before spraying. It is evident that both σ_0 and σ_N are strongly influenced by the crack length and the pin radius, and thus cannot be used as a universal index of the adhesive strength of the coating-substrate couple.

Figure 7 shows the test data expressed by the stress intensity factor at failure K_{Int}. The values were obtained

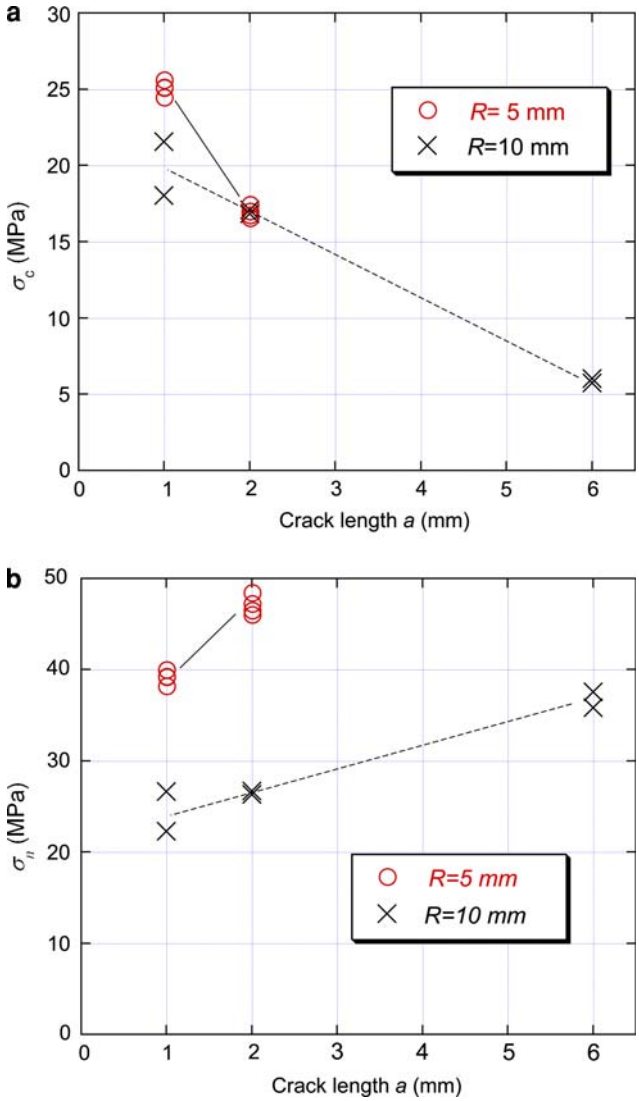

Fig. 6 (a) Results of tensile test expressed in terms of apparent average stress σ_0 and crack length a. (b) Results of tensile test expressed in terms of stress over the unmodified interface σ_n and crack length a

by substituting the experimentally determined σ_c and F_I (a/R) in Fig. 4 into Eq. 1. The results indicate that the coating-substrate interface failed when the stress intensity factor at the interface reached approximately 2 MPa $m^{1/2}$ in the present study regardless of the differences in the geometry of the test specimens. More precisely, the interfacial toughness K_C calculated from the data in Fig. 7 was 1.9 ± 0.1 MPa $m^{1/2}$. Therefore, interfacial toughness as determined by the present procedure can be a meaningful parameter to characterize the adhesion of thermal-sprayed coatings.

A possible source of errors in the toughness value is the estimated Young's modulus of the coating. Recently, Watanabe et al. reported a work containing information about the effects of elastic modulus of the coating (Ref 25). The effects of E_c/E_b on the correction factor F_I for different values of normalized crack length a/R were

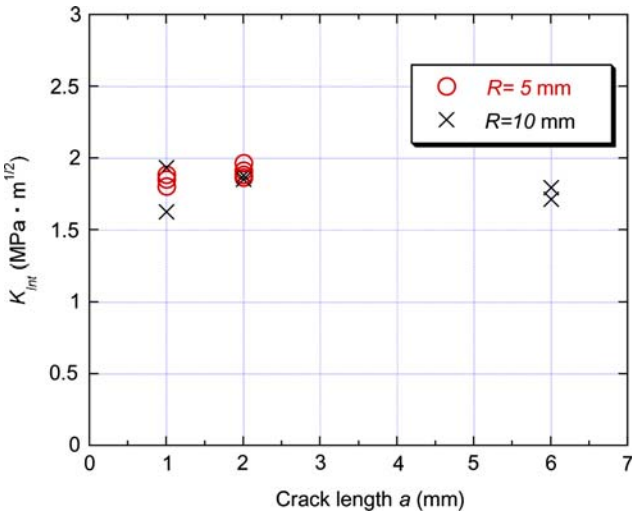

Fig. 7 Results of tensile test expressed in terms of stress intensity factor K_{Int} and crack length a

calculated using FEM. Even though it deals with straight tensile test specimens with a circumferential crack and thus the geometry is different from the present case, the degree of influence of E_c/E_b on F_I should be comparable. Based on these data, the error in toughness corresponding to an uncertainty of the elastic modulus ratio of the coating to the substrate $E_c/E_b = 0.5 \pm 0.2$ is estimated to be ±10% approximately.

Since the interfacial toughness of thermal-sprayed coatings depends on the thermal-spray process, coating and substrate materials, substrate pretreatment, as well as the mode mixity, various interfacial toughness values have been reported. For plasma-sprayed coatings fabricated in air atmosphere, Inoue reported values of about 0.5 and 1.25 MPa $m^{1/2}$ for CoNiCrAlY and Ni-20Cr coatings made on cast iron substrates (Ref 20). For HVOF-sprayed 316L stainless steel coatings on carbon steel substrates, Watanabe showed that the toughness changes from almost 0 to 7 MPa $m^{1/2}$ by changing the substrate surface roughness and preheating temperature (Ref 19). For HVOF-sprayed, WC-Co cermet coatings, toughness increased significantly with the increase in WC grain size from 13 to 22 MPa $m^{1/2}$ (Ref 19).

Chicot reported toughness values from 4 to10 MPa $m^{1/2}$ for HVOF-sprayed Cr_3C_2-NiCr on various substrates (Ref 14). For vacuum plasma-sprayed titanium coatings on Ti-6Al-4V substrates, Howard reported a value of 0.8 MPa $m^{1/2}$ (Ref 10). The present result is in a reasonable range as compared to these previously reported results, but it should be sensitive to the parameters stated above.

5. Conclusion

A newly designed pin-test specimen with a circumferential precrack has been applied to evaluate adhesion of plasma-sprayed stainless steel coatings and the following results were obtained.

(1) It was shown that a newly designed test specimen with a circumferential precrack could preserve the critical geometry during grit-blasting and plasma-spraying procedures.

(2) The correction function F_I is a function of a dimensionless parameter a/R.

(3) Although the failure stress σ_c calculated over the total surface area or σ_n calculated over the unmodified interface area in the pin test strongly depended on the specimen size and the precrack length, interfacial toughness was rather constant at 1.9 ± 0.1 MPa $mm^{1/2}$ regardless of the varied geometrical parameters.

As a consequence, this testing procedure can be considered as a viable method to evaluate adhesion of thermal-sprayed coatings.

Acknowledgments

We express our appreciation to Messrs. M. Komatsu, T. Ono, and H. Yamada at the National Institute for Material Science for their useful advice and technical assistance.

References

1. S. Kuroda, J. Kawakita, T. Fukushima, and S. Tobe, Importance of the Adhesion of HVOF Sprayed Coatings for Aqueous Corrosion Resistance, *Mater. Trans.*, 2003, **44**(3), p 381-388
2. T. Sundararajan, S. Kuroda, F. Abe, and S. Sodeoka, Effect of Thermal Cycling on the Adhesive Strength of Ni-Cr Coatings, *Surface Coat. Technol.*, 2005, **194**, p 290-299
3. M.F. Bahbou, P. Nylén, and J. Wigren, Effect of Grit Blasting and Spraying Angle on the Adhesion Strength of a Plasma-sprayed Coating, *J. Thermal Spray Technol.*, 2004, **13**(4), p 508-514
4. V. Pershin, M. Lufitha, S. Chandra, and J. Mostaghimi, Effect of Substrate Temperature on Adhesion Strength of Plasma-sprayed Nickel Coatings, *J. Thermal Spray Technol.*, 2003, **12**(3), p 370-376
5. P. Fauchais, A. Vardelle, M. Vardelle, and M. Fukumoto, Knowledge Concerning Splat Formation: An Invited Review, *J. Thermal Spray Technol.*, 2004, **13**(3), p 337-360
6. S. Kuroda, T. Fukushima, and S. Kitahara, Significance of Quenching Stress in the Cohesion and Adhesion of Thermally Sprayed Coatings, *J. Thermal Spray Technol.*, 1992, **1**(4), p 25-332
7. C.K. Lin and C.C. Berndt, Measurement and Analysis of Adhesion Strength for Thermally Sprayed Coatings, *J. Thermal Spray Technol.*, 1994, **3**(1), p 75-104
8. L.W. Crane, C.L. Johnston, and D.H. James, Effect of Processing Parameters on the Shear Adhesion Strength of Arc Sprayed Deposits, *Proc. 10th Int. Thermal Spraying Conf., DVS*, Germany Welding Society, Dusseldorf, Germany, 1983, p 46-50
9. M. Fukumoto, H. Murakami, I. Okane, and H. Harada, Improved Ring Shear Test for the Evaluation of Adhesion Strength of Thermal Sprayed Coating, *Nippon Kinzoku Gakkaishi (J. Japan Inst. Metal)*, 1995, **59**(1), p 84-88, (in Japanese)
10. S.J. Howard and T.W. Clyne, Interfacial Fracture-Toughness of Vacuum-Plasma-Sprayed Coatings, *Sur. Coat. Technol.*, 1991, **45**(1-3), p 333-342
11. M. Sexsmith and T. Troczynski, Peel Adhesion Test for Thermal Spray Coatings, *J. Thermal Spray Technol.*, 1994, **3**(4), p 404-411
12. C.C. Berndt and R. McPherson, A Fracture Mechanics Approach to the Adhesion of Flame and Plasma Sprayed Coatings, *Proc. 9th Int. Thermal Spraying Conf.*, Amsterdam, 1980, p 310-316
13. P. Ostojic and R. McPherson, Determining the Critical Strain Energy Release Rate of Plasma-sprayed Coating Using a Double-cantilever-beam Technique, *J. Amer. Ceramic Soc.*, 1988, **10**, p 891-899
14. D. Chicot, P. Démarécaux, and J. Lesage, Apparent Interface Toughness of Substrate and Coating Couples from Indentation Tests, *Thin Solid Films*, 1996, **283**(1), p 151-157
15. J. Lesage and D. Chicot, Role of Residual Stresses on Interface Toughness of Thermally Sprayed Coatings, *Thin Solid Films*, 2002, **415**(1), p 143-150
16. ISO 14916:1999, *Thermal Spraying—Determination of Tensile Adhesive Strength*, ISO/TC 107
17. ASTM C633-01, Standard Test Method for Adhesion or Cohesion Strength of Thermal Spray Coatings, American Society of Testing Materials, Philadelphia, 2001
18. JIS H 8402:2004, *Test Methods of Tensile Adhesive Strength for Thermal-Sprayed Coatings*. Japanese Standards Association, Tokyo (in Japanese)
19. M. Watanabe, A. Owada, S. Kuroda, and Y. Goto, Effect of WC Size on Interface Fracture Toughness of WC-Co HVOP Sprayed Coatings, *Surface Coat. Technol.*, 2006, **201**(3-4), p 619-627
20. Y. Inoue, T. Ono, A. Noutomi, A. Izuha, M. Toyoda, and M. Tsukamoto, Adhesive Strength Evaluation of Plasma Sprayed Coatings by Tensile Pin Test, *Quart. J. Jpn Weld. Soc.*, 1991, **9**(1), p 167-173, (in Japanese)
21. A. Kishi, S. Kuroda, T. Fukushima, and T. Inoue, Adhesive Strength Evaluation of HVOF Thermal Sprayed Coatings by Tensile Pin Test, *Preprint Natl Meet. Jpn Weld. Soc.*, 2001, **69**, p 212-213, (in Japanese)
22. G. Qian, T. Nakamura, C.C. Berndt, and S.H. Leigh, Tensile Toughness Test and High Temperature Fracture Analysis of Thermal Barrier Coatings, *Acta Mater.*, 1997, **45**(4), p 1767-1784
23. R. Yuuki, Kaimen No Rikigaku (Mechanics of Interface). Tokyo, Baifuukan Co., Ltd, 1993, p 91-105, (in Japanese)
24. S. Kuroda and T.W. Clyne, The Quenching Stress in Thermally Sprayed Coatings, *Thin Solid Film*, 1991, **200**(1), p 49-66
25. M. Watanabe, S. Kuroda, K. Yokoyama, T. Inoue, and Y. Gotoh, Modified Tensile Adhesion Test for Evaluation of Interfacial Toughness of HVOF Sprayed Coatings, *Surf. Coat. Technol.*, 2008, **202**(9), p 1746-1752